DETERMINING THE RADII OF QUANTUM NANO-PARTICLE SEMICONDUCTORS WITH FLUORESCENCE SPECTROSCOPY

A PREPRINT

Nathan C. Pierce
Department of Physics (Undergraduate)
University of Michigan - Dearborn
4901 Evergreen Rd, Dearborn, MI 48128
piercen@umich.edu

March 29, 2021

ABSTRACT

In this experiment, collected spectra is used to determine the radius of four differently sized nano-particle indium phosphide (InP) semiconductors by exploiting the process of fluorescence, and are: $R_{red} = (2.9 \pm 0.3)\,\mathrm{nm}$, $R_{orange} = (2.7 \pm 0.3)\,\mathrm{nm}$, $R_{yellow} = (2.5 \pm 0.3)\,\mathrm{nm}$, $R_{green} = (2.4 \pm 0.3)\,\mathrm{nm}$. Each radius is determined by using the discretized energy equation for quantum system in a 3-dimensional infinite square well potential in conjunction with the measured peak-wavelength value of each quantum dot spectra. In the process, spectrometer calibration is completed and used to transform spectra pixel number data to a wavelength, and the β-line of the Balmer series of Hydrogen is examined. A two-peak Gaussian best fit curve is generated for the β-line data.

1 Introduction

The conclusion of this experiment is the deduction of the nano-particle radii, but there are several tasks completed in the interim. These include (in order):

1. Understanding the set-up and use of the Ocean Optics USB4000 spectrometer (and spectrometer technology in general).
2. Understanding the calibration process by checking measured spectra against the known peak wavelengths of a mercury vapor lamp.
3. Measure the spectra of various light sources such as a neon laser, excited H_2 and deuterium gas.
4. Transform the spectra of these sources using the calibration equation and coefficients determined during the calibration process from the raw pixel number data to wavelength, and check the transformation against the measured Wavelength vs. Intensity spectra from the same light source.
5. Obtain the emission spectra of the Cenco quantum dots and use the peak wavelengths to determine their size (radius).

The discussion in the Methods and Results sections follow this sequence of ideas. Both of these sections contain matching subsections so that the discussion can be easily followed and referenced.

Since a range of topics in physics is touched upon throughout the course of the experiment, a fair amount of theory is needed to develop the intuition in understanding what is happening. These topics include: spectroscopy, line emission spectra (particularly the Balmer series of hydrogen), some basic quantum theory (Schrödinger equation, particle in a box), and solid-state semiconductor theory. The quantum dots are semiconductors made of indium phosphide (InP). As a quick check, the given band gap energy of the semiconductor by Cenco is $E_g = 2.15 \times 10^{-19}$ J, which matches the band gap energy of InP.

2 Theory

The experiment touches on a number of important topics in physics, so a brief recap on the theory of these topics are provided below, and includes: 1-dimensional wavefunctions and potential wells, semiconductors, emission line spectra, and spectroscopy.

A quantum system's state is described by the Schrödinger equation. In this case, we can restrict our application to use the time independent Schrödinger equation (TISE). The Schrödinger equation is:

$$i\hbar\frac{\delta\Psi}{\delta t} = \frac{\hbar^2}{2m}\frac{\delta^2\Psi}{\delta x^2} + V\Psi \tag{1}$$

The right hand side of this equation is often referred to as the Hamiltonian of the wavefunction Ψ. Ψ is generally a function of some spatial coordinates in Euclidean space ($\hat{x}, \hat{y}, \hat{z}$, for example), and as a function of time, t. We have already assume time-independence, and we'll restrict analysis further to one dimension (say x).

The Hamiltonain is an operator, which when applied to a wavefunction, yields energy state eigenvalues:

$$\hat{H}\Psi = E\psi \tag{2}$$

E is a separation constant, that must exist in order to make Eq. 1 true. If the wavefunction is known, applying the Hamiltonian to it allows us to measure a physical property of the quantum system - its energy. Energy is called an *observable*. Preceding further into the theory puts us in to formalism that is not needed for understanding the experiment, but it is important to understand how the mathematical theory develops into a physical one, as is directly represented by Eq 2.

For a stationary state, we can write the potential independently of time, as in the case above. Because the quantum dot experiment is meant to showcase the macroscopic properties of a quantum system, namely, a system which is free of potential within certain bounds, concepts developed from the classic particle in a box scenario are needed in order to understand what exactly is happening.

For the particle in a box, infinite potentials are established at $x = 0$ and $x = L$, where L is some arbitrary distance. Here, the potential is solely a function of position: $V = V(x)$. Inside the boundaries, the particle is free.

$$V(x) = \begin{cases} 0, & 0 \leq x \leq L \\ \infty, & otherwise \end{cases} \tag{3}$$

The particle cannot exist outside of these boundaries - the wavefunction at the boundaries must be zero, i.e. $\Psi(0) = \Psi(L) = 0$. The probability of finding the particle outside of the well is $|\Psi|^2 = 0$.

[1]Griffiths, "Introduction to Quantum Mechanics, 3rd E."

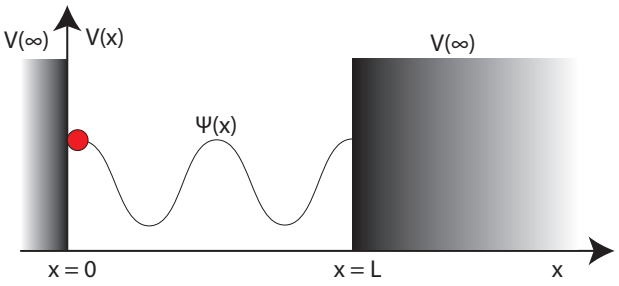

Figure 1. The classic particle in a box. Infinite potentials exist outside of the box - clasically, the particle can not exist outside of the box. The location of the particle is a normalized distribution $|\psi|^2$ from $x = 0$ to $x = L$. Note that inside these bounds, there is no potential - the particle is free. In the quantum dot experiment, the boundaries are established by the size of the dot - the 3-dimensional R in Eq 9 corresponds to the 1-dimensional L pictured here.

With a zero potential $V = 0$, Eq 2 becomes:

$$\frac{d^2\Psi}{dx^2} = -k^2 \tag{4}$$

Here, $k = \frac{\sqrt{2mE}}{\hbar}$. This ordinary differential equation is the same as a simple harmonic oscillator, which has the solutions:

$$\Psi(x) = Asin(kx) + Bcos(kx) \tag{5}$$

The solution for the particle in a box thought experiment can be refined by applying the boundary conditions, $\Psi(0) = \Psi(L) = 0$. Doing so allows us to find the definite total energy of the particle:

$$E_n = \frac{\hbar^2 k^2}{2m} = \frac{n^2\pi^2\hbar^2}{2mL^2} \tag{6}$$

The parameter n refers to the energy state of the particle, with $n = 1$ being the ground state (note n is a positive integer). Energies beyond the ground state increase in proportion to n^2 and are the nth excited states of the particle.

From the particle in a box situation, three important properties of a quantum system are deduced[1]:

1. The energy of a particle has a discrete, quantized energy.
2. The lowest energy state ($n = 1$) of a particle is non-zero.
3. For some positions along L, there are nodes where the particle will never be found.

When a particle absorbs energy, electron(s) are excited to higher orbitals. In the case of the experiment, energy is transferred to the system (nanoparticles) via photons

from an LED. These electrons tend towards a lower, more stable energy, and will transfer down to these lower energies. In this process, a photon is emitted (a process called florescence), with energy equal to the energy difference:

$$E_{photon} = \hbar f = \Delta E_{electron} = E_{upper} - E_{lower} \quad (7)$$

We can measure E_{photon} easily with a spectrometer, by measuring the wavelength with peak intensity in the spectrum and using the relation $E_{photon} = \frac{hc}{\lambda}$. Every element will emit a characteristic set of wavelengths based on the atomic structure. Therefore, the material composition of a sample can be determined by studying its emission spectra. When fitting data of the emission spectrum of some material, it is common to use either a Gaussian, Voight, or Lorentzian distribution. The distinguishing features of these functions is the behavior of the tales. All things being equal, the Lorentzian function tends to decay more slowly, and a Gaussian decays from the peak most rapidly.

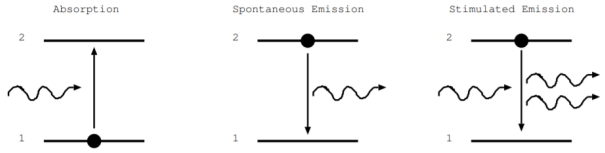

Figure 2. Diagrams showing the processes of absorption and emission of photons. The black dot is an electron, which in the left case is being excited by the absorption of an incident photon. If the incident photon contains enough energy, the electron in the lower energy state will transition to the higher level. In the middle, such a transition has already occurred, and the electron is transitioning down to a lower energy state spontaneously - in the process, emitting a photon. The right diagram shows stimulated emission, which occurs when a photon is incident on an electron already in an excited state - the emitted photon is the combined energy of the excited state and incident photon energy. Source: Engineering LibreTexts

A quantum system can absorb energy (and therefore emit photons) in many different ways, but in this experiment, the system (dots) are subject to electromagnetic radiation impingement in the form of a $405\,\mathrm{nm}$ LED. This specific type of spectroscopy is called fluorescence spectroscopy.

Figure 3. The Balmer series for H_2. The α-peak is the red line, and the β-line (analyzed in the experiment) appears as the first peak to the left of it. Note that six peaks are visible, but the two left-most peaks are considered ultraviolet, despite the fact that they can be seen by the naked eye. Source: Jan Homann Photography

[2]Krane, "Modern Physics", 3rd E.

In the experiment, the Balmer series of H_2 gas is examined. The Balmer series is one of a set of six spectral line series of hydrogen (See Fig 3 for a photograph of it). They are of particular interest because the emission lines are within the visible light range. The four peak wavelengths occur at $410\,\mathrm{nm}$ (δ lines), $434\,\mathrm{nm}$ (γ lines), $486\,\mathrm{nm}$ (β lines), and $656\,\mathrm{nm}$ (α lines). The Rydberg equation is a generalization of the Balmer formula, and for hydrogen has the form:

$$\frac{1}{\lambda_{vac}} = R_H(\frac{1}{n_1^2} - \frac{1}{n_2^2}) \quad (8)$$

Where λ_{vac} is the wavelength of the light emitted in vacuum, R_H is the Rydberg constant (for H_2,$R_H \approx 1.096 \times 10^7\,\mathrm{m}^{-1}$), and n_1 and n_2 are the principal quantum numbers (excited states) of the transition. The energy can be found by using the relation $E = \frac{hc}{\lambda}$.

Now, the particle in a well experiment yielded some very interesting results, but it is not applicable to semiconductors. Since the experiment uses semiconductors, some extra concepts are needed. The quantum dots are solids, and contain many electrons. The atoms in the solid lattice are arranged in regular, periodic patterns. In such a system, where the number of atoms N is very large, the electrons split into discrete energy bands that correspond to the energy levels previously described (recall that the Pauli Exclusion principle restricts the number of electrons per energy level to two - and they must have opposite spins). Except now, there are some multiple of N unique energy levels, each with $2N$ electrons (thus the idea of a 'band'). Same as before, no electron is permitted to have energy within the energy bands.

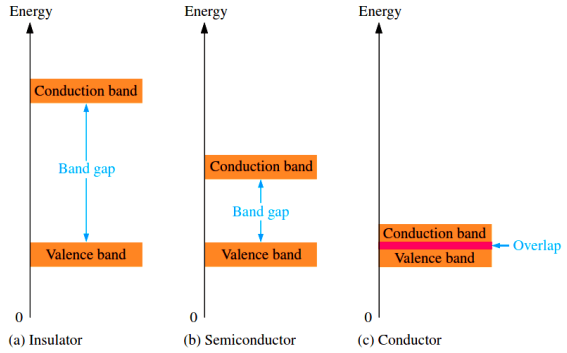

Figure 4. Some of the electrical properties of solid materials is determined by the magnitude of the band gap. This diagram shows how the size of the band gap determines the conductivity of a material - an insulator (left), semiconductor (middle), and conductor (right). Source: Instrumentation Tools

There are two energy bands of interest: the conduction band, and the valence band, which are determined by the Fermi level, E_F [2] (the [2] is a footnote mark). For semiconductors, the energy gap E_g is around $1\,\mathrm{eV}$. Valence

electrons can transition from the top-most valence band to the outermost level - the conduction band, but no electrons can exist between the two bands. The energy required for this transition is the band gap energy, E_g. See Fig 4 for an illustration of the band gaps for different materials.

There are two charge carriers that transition between the bands: the electron, and a quasiparticle called a hole. A hole is the absence of an electrons. Holes can move through the solid lattice just as electrons can. Both holes and electrons contribute to the electrical conductivity of a solid.

Since the quantum dot is a semiconductor, the quantum system is composed of an electron and a hole. The energy of the nanoparticle is the summation of the energy of the electron and hole in the semiconductor, as well as the band gap energy E_g. Additionally, the particle exists in three dimensions, and the "well" is spherical in shape rather than square. If the wavelength of the photon with energy E is measured, then the size of the particle can be solved. The energy of the photon emitted by the florescence of the quantum dot is:

$$E = \frac{\hbar^2\pi^2}{2m_eR^2} + \frac{\hbar^2\pi^2}{2m_hR^2} + E_g \tag{9}$$

Here R is the radius of the dot, m_h is the mass of the hole ($m_h = 5.47 \times 10^{-31}\,\text{kg}$), m_e is the mass of the electron ($m_e = 7.29 \times 10^{-32}\,\text{kg}$), and E_g is the band gap energy $E_g = 2.15 \times 10^{-19}\,\text{J}$.

3 Methods

There were a number of tasks performed before the quantum dots were analyzed. In order, they are: use the spectrometer to obtain the spectra of a calibration source (mercury lamp) and use it to calibrate the spectrometer, use the calibrated spectrometer to transform the spectra of the source to wavelength and check against the true values, record the spectra of various light sources (neon laser, excited hydrogen gas, deuterium), collect spectra of the quantum dots, and finally determined the radius of the dots from the peak emission wavelengths (using Eq 9).

3.1 Experimental Setup

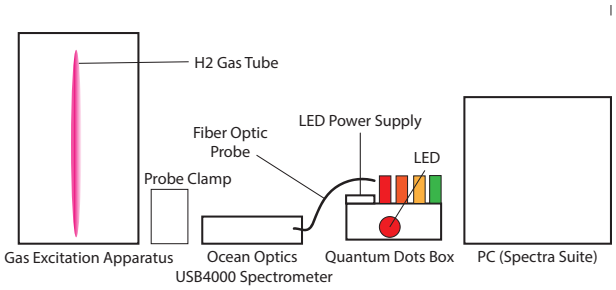

Figure 5. The set up of the experiment. Not pictured are the other gas tubes, neon laser, and the mercury lamp.

Before details on the processes are discussed, the set up of the experiment is laid out. The spectrometer used is a Ocean Optics USB4000 spectrometer, which received its input from a fiber optic probe ($50\,\mu\text{m}$). Care was taken to keep the probe cable straight (no kinks in the line). The quantum dot box had a small hole drilled into the side which could be used to keep the probe secure and to reduce the collection of ambient light while measuring the spectra of the dots. A clamp was used to keep the probe in position while measuring other light sources, such as excited hydrogen gas from the gas excitation apparatus. The dots themselves (see Fig 6) could be moved along a divot in the quantum dots box. A hole was drilled into the bottom of the divot for the $405\,\text{nm}$ LED light to illuminate the dot vials. Only one vial could be illuminated at a time with this configuration. The container holding the vials had an exposed bottom which allowed the light from the LED through. A various assortment of gas tubes were available for use with the gas excitation apparatus. Care was taken to not run the apparatus for more than 30 seconds. The USB spectrometer was connected to a PC running Spectra Suite spectroscopy software. The mercury lamp used in the calibration process was housed in a metal box with a small circular window to allow probing of its emission. Care was taken here to prevent human exposure to this light.

Figure 6. The quantum dot nano-particles used in the experiment. The particles are InP molecules suspended in a liquid solution. In each vial, the material is the same, but the size of the particle differs. The color emitted is a function of this size. Source: Cenco

3.2 Calibration

The first task in the experiment was to become familiar with the spectrometer and spectrometer software by going through the calibration process. A mercury vapor lamp was used as the calibration light source. The optical probe was clamped in the window of the lamp's window to allow spectral collection. First, the Spectra Suite software was placed into scope mode, the X-axis was changed to Pixel count, and the integration time was adjusted (to within milliseconds) to allow for several peaks in the emission but prevent the intensity of the peaks from exceeding the scale of the Y-Axis, which capped at around 60,000 (counts).

The pixel number of a peak could be found by moving the cursor to a peak and clicking at the maximum. The pixel numbers for all peaks were recorded. Each recorded data entry should correspond to a true peak wavelength for mercury, which was collected from the NIST atomic spectra database.

The calibration equation given by the manufacturer is a cubic polynomial:

$$\lambda_p = I + C_1 p + C_2 p^2 + C_3 p^3 \tag{10}$$

Where λ_p is the wavelength of pixel number p, and I is the wavelength of pixel 0.The goal was to fit the pixel number data collected to this equation in order to determine the calibration coefficients C_1, C_2, C_3. The SciPy curve_fit() function was used to find the calibration coefficients. Then, the curve fit routine was run a second time to find the slope and Y-intercept of the Pixel Number vs. True Wavelength graph. A plot of this graph should be linear for a calibrated spectrometer (R-square value very near 1). If it is not, then the calibration coefficients can be updated for the spectrometer.

3.3 Spectra Transformation

After the calibration process, the spectra of the mercury lamp was transformed from pixel number to wavelength. This was accomplished by collecting data of Pixel Number vs. Intensity, and passing the pixel number data through the calibration equation (Eq 10) using the calibration coefficients C_1, C_2, C_3, and I determined in the first part. Then, another spectra sample was collected but this time the X-Axis data was changed back to wavelength. To compare the accuracy of the coefficients and the calibration equation (Eq 10), the two plots were overlaid on the same graph. Ideally, the two graphs should be nearly indistinguishable.

3.4 Hydrogen Emission Lines

Now confident that the spectrometer was calibrated, the emission line spectra of excited H_2 gas was examined. The fiber optic probe was clamped to a stand, and placed near the gas excitation apparatus with a tube of hydrogen gas inserted. Turning the apparatus on results in the excitation of the hydrogen molecules, which is clear by the pinkish optical light given off.

Once the spectra was collected, a custom curve fitting Python widget was used to fit the data to a Gaussian curve and generate a best guess of the fit parameters for the β-line of the hydrogen ($486\,\mathrm{nm}$). As discussed in Sec 4, a single Gaussian peak did not fit the data well, so a Lorentzian fit was attempted, and finally a two-peak Gaussian fit. A line was also added to the fit function. The best-guess parameters from the best fit widget were passed against to SciPy's curve_fit() routine, which generated the fit parameters with an associated uncertainty.

3.5 Quantum Dots

The final component of the experiment is collecting the spectra of the four differently sized Cenco quantum dots, and using Eq 9 to solve for the radius. Spectra was collected for each of the four quantum dot vials. The energy for each peak wavelength was determined using $E = \frac{hc}{\lambda_{peak}}$. This is the E term that appears on the left hand side of Eq 9. Then, solving for the radius is straightforward.

4 Results and Discussion

As with the methods section, the discussion of experimental results follows the chronological order of sub-experiments.

4.1 Calibration

The calibration coefficients C_1, C_2, C_3 from Eq 10 were found to be $C_1 = (2.6 \pm 0.6) \times 10^{-1}$, $C_2 = (-5.6 \pm 0.6) \times 10^{-5}$, and $C_3 = (1.5 \pm 1.8) \times 10^{-8}$. The slope of the linear calibration curve for True Wavelength vs. Pixel Number is $k = 0.203 \pm 0.003$. Fig 7 shows this plot. The data shows a strong linear trend - as would be expected for a calibrated spectrometer. It is evident that the Ocean Optics spectrometer does not need calibration. This allows for a higher confidence of the results obtained going forward. There is one peculiar point near the 600 pixel number point which appears to be an outlier. The point was not excluded from the fit.

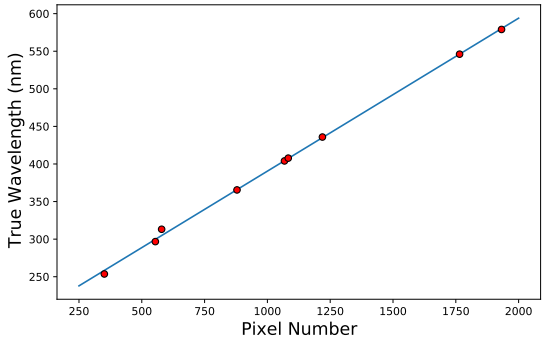

Figure 7. The four NanoSys Quantum Dot vials used in the experiment. Each vial contains quantum dots of slightly different sizes. A strong illuminating sources was likely used in this photo in order to achieve fluorescence (without which the vials would not have a distinct color as they do in the photo). The slope of the line is $k = 0.203 \pm 0.003$. There is one point of interest - the third point from the origin, near the 600 pixel number mark. Source: Cenco Phyics/NanoSys Quantum Dots Manual

λ_T (nm)	Pixel Num	λ_p(nm)	Difference
253.65	351	255.10	-1.46
296.72	554	300.31	-3.59
313.16	579	305.68	7.48
435.83	1219	434.88	0.9
546.08	1765	544.33	1.75
578.97	1932	580.15	-1.18

TABLE I. A portion of the data collected for determining the calibration coefficients for Eq 10, C_1, C_2, C_3 from the spectra of a mercury lamp. λ_T is the true wavelength determined from the NIST database, and λ_p is the predicted wavelength, generated by solving the calibration equation with the coefficients produced from the best fit routine. This data was used in generating the graph of Fig 7. The difference column shows $\lambda_P - \lambda_P$.

4.2 Spectra Transformation

The calibration coefficients C_1, C_2, C_3, and I were used along with Eq 10 to transform data in the form Pixel Number vs. Intensity to the form Wavelength vs. Intensity. A plot of this transformed Wavelength vs. Intensity data was plotted against a separate collection of data in the form of Wavelength vs. Intensity (from the same light source). The purpose of this was to verify that the calibration equation, and the calibration coefficients, are correct. If they are correct, the two plots should overlap one another, with peak wavelength locations at the same point along the X-axis. This graph is Fig 8.

Visual inspection of the graph shows that the transformed spectra is certainly representative of the directly sampled spectra, but there are some noticeable discrepancies between the exact peak wavelength locations, especially between the 300 nm and 400 nm range. Throughout the experiment, it was typical to see a difference in the magnitude of the *intensity* for a given peak wavelength between spectras of the same samples, but the peak wavelength location should *not* differ, so the fact that the lines are represented by two completely different data sets should not matter in consideration of the peak wavelength locations. It is interesting that the range of of data (300 nm - 400 nm) that is off in this graph is also the range of data from the collected calibration data (Table I) that has the greatest difference $\lambda_P - \lambda_P$. In reality, this should not matter, as the calibration coefficients ought to produce an accurate transformation of the pixel number to wavelength for the whole converted data set. The exact cause of this discrepancy is unknown, but may be related to a parameter used in the sampling software called the boxcar width, which is a data smoothing technique that averages a group of adjacent detector elements. The boxcar width setting used for this sample was 5, which means each data point is averaged with the 5 points to the left and right of the point. While the signal to noise ratio is improved with increasing boxcar width, it may affect the smaller peak wavelengths, as the averaging affect has greater impact on the smaller peaks.

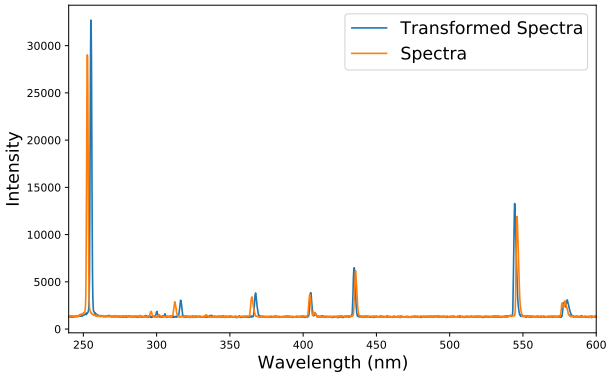

Figure 8. Emission spectra of the mercury vapor lamp. The blue line is the transformed spectra (from pixel number to wavelength), and the orange line is the directly sampled Wavelength vs. Intensity data. The wavelength peak location discrepancy for the 300 nm - 400 nm may be related to a Spectra Suite sampling option called boxcar width.

4.3 Hydrogen Emission Lines

A few complications occurred in fitting the β-line wavelength peak of H_2. First, a single Gaussian peak did not fit the data well - specifically, the behavior near the start of the exponential increase in intensity. In light of this, a Lorentzian curve was attempted, but a similar issue was encountered. Finally, a two-peak Gaussian function was used to fit the data, which fit the data well. The peak of the β-line was asymmetric - the left side of the peak did not fit the single-peak Gaussian fit (the addition of the second Gaussian peak corrected this). See Fig 9 for the plot. This could be an issue related to the resolution of the spectrometer, or possibly a unique feature of the β-line. Without looking at the other peaks in the Balmer series, it is hard to

say. To probe further into this issue, the first step should be to use a higher quality spectrometer with greater resolution. Another possibility is that the H_2 sample may have been compromised somehow - perhaps there are other atomic species within the tube. The data, two-peak Gaussian fit, and the individual Gaussian fit peaks are shown in Fig 9.

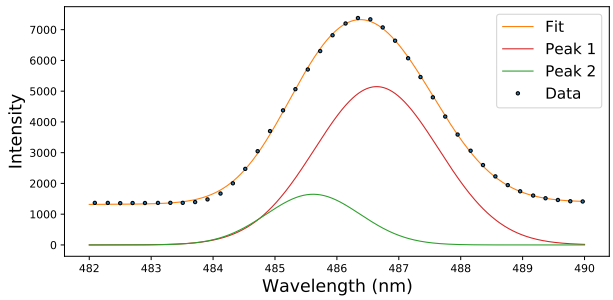

Figure 9. The data and best-fit curve for the β-line of the Balmer series of H_2. The data (black dots), best-fit curve (orange), and Gaussian peaks appearing in the fit-function (red and green) are superimposed on one image to show how two Gaussian peaks best fit the data. While spectra showing all four lines of the Balmer series of Hydrogen was collected, only the β-line was analyzed. A single peak Gaussian and a Lorentizan were used in an attempt to find the best fit, but neither of these worked well. The orange curve is a two-peak Gaussian (components shown in red and green).

Another issue encountered in this portion of the experiment was peaking of the intensity for different samples with the spectrometer for different wavelength peaks. It was common throughout the experiment to get wavelength peaks of disproportionate intensity - some peaks had much greater intensity than others. This could cause the peak to 'flatten' at the maximum allowed intensity of the spectrometer (around 60,000 counts). The problem could easily be resolved by lowering the integration time, but this had it's own problems, since lowering trhe integration time could potentially (and did) remove some of the lower intensity peaks entirely from the spectra. Care was taken to adjust the integration time until a workable balance was struck - such a integration time that a peak did not exceed the maximum plotable intensity, but one which also did not remove some of the lower intensity peaks of interest.

4.4 Quantum Dots

Extracting the energy for each peak wavelength of each quantum dot is straightforward (see Sec 3 for details). Each peak wavelength has excitation energy equivalent to $E = \frac{hc}{\lambda_{peak}}$ - this value is equivalent to E (the left-hand side) in Eq 9, and are plotted in Fig 10. The results (quantum dot sizes) are presented in Table II.

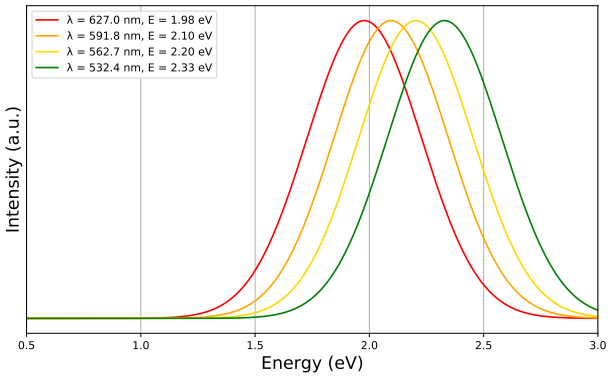

Figure 10. The Gaussian curves (with arbitrary units) corresponding to the measured peak wavelengths from the spectra of the quantum dots. Note that the measured room ambient temperature at the time of measurement was 295.8 K.

The results for the peak wavelength differ slightly from the values given in the lab manual (see Fig 11). Evidently, the small disparity in peak wavelengths between what was obtained experimentally and the accepted values from Cenco is not enough to disrupt the accuracy of the radii determined experimentally, at least for the level of precision given. Since the values of peak wavelength differ slightly, it should be expected that the values of the radii also differ as precision for each radius grows. But, for the uncertainties determined, the values for the radii agree with the Cenco values. The experimental results (Table II) and the accepted values from Cenco (Fig 11) are placed together for easy comparison.

Dot Color	λ_{peak} (nm)	Radius (nm)
Red	626.9 ± 1.5	2.9 ± 0.3
Orange	591.8 ± 1.5	2.7 ± 0.3
Yellow	562.7 ± 1.5	2.5 ± 0.3
Green	532.4 ± 1.5	2.4 ± 0.3

TABLE II. The experimental results for the radii of the quantum dots determined from the emitted photon energy. The peak wavelengths λ_{peak} differ slightly from those given by Cenco (Fig 11), but this small difference still allows for an accurate determination of the radii for the precision given, as the results obtained experimentally for the radii do agree with those given by Cenco.

Actual sizes and Peak Wavelengths:

Color	Peak Wavelength (nm)	Radius (nm)
Green	540	2.367454
Yellow	570	2.533894
Orange	600	2.718174
Red	630	2.924941

Figure 11. The reported peak wavelengths and nano-particle radius for each quantum dot, provided in the Cenco instructors manual.

5 Conclusion

The experiment was a success based on the deduced values of the quantum dot radii matching the provided Cenco values. The quantum dot experiment showcases the effectiveness of quantum theory in a macroscopic manner (i.e., it is easy to see quantum effects by the emission of different peak wavelengths as a function of the semiconductor size). The quantum theory encompasses a wide-range of topics, including radiation and emission line spectra, the Schrödinger equation and the square well potential (more importantly - what results from it), and semiconductor physics. Furthermore, it was interesting to collect and analayze the spectra of various light sources, compare them against the true wavelengths (provided by the NIST database), and generate the calibration coefficients for the cubic polynomial calibration equation using spectra from a mercury vapor lamp. While the peak wavelengths measured for the quantum dot spectra differed slightly from the values provided by Cenco, the agreement between values obtained for the radii is promising.

References

[1] Griffiths, David Jeffrey, and Darrell F. Schroeter. Introduction to Quantum Mechanics. Cambridge University Press, 2019.

[2] Modern Physics, by Kenneth S. Krane, 3rd ed., Wiley, 2020, pp. 326–357.

[3] Operating Instructions, 1751-18 CENCO Quantum Dots Lab Manual

[4] Homann, Jan. "Balmer Series." Wikipedia, Wikimedia Foundation, 17 Feb. 2021, en.wikipedia.org/wiki/Balmer$_s eries/media/File$: $Visible_s pectrum_o f_h ydrogen.jpg$.

[5] Mitofsky, Andrea M. "7.1: Absorption, Spontaneous Emission, Stimulated Emission." Engineering LibreTexts, Libretexts, 22 Mar. 2021.

[6] "Band Gap for Semiconductor Materials." Instrumentation Tools, 5 Oct. 2016, instrumentationtools.com/band-gap/.